北見工業大学研究報告
第18巻 第1号 (昭和61年)

Memoirs of the Kitami Instisute of Technology
Vol. 18 No. 1 (1986)

Computer Simulation of Ozone Electrosynthesis in an N_2/O_2 Mixture-fed Ozonizer*

by Kousaku YOSHIDA** and Hiroaki TAGASHIRA***

(Received April 30, 1986)

Abstract

A computer simulation was performed to study the process of ozone electrosynthesis in the silent dicharges in N_2/O_2 mixtures. The simulation model based on continuity equations for reaction particles and on Poisson's equation was employed, in which 34 reactions in the gases and two secondary processes at the cathode were considered.

The optimum yield efficiencies of ozone at various mixture rates obtained by the simulation are in good agreement with the experiment and it is shown that the dissociation of oxygen molecules by excited nitrogen molecules successfully explains why the ozone efficiencies in the gas mxtures are higher than those estimated from only the O_2 fraction. The ozone generation process in air is discussed in detail. The temporal and spatial variations of the electron density and the electric field intensity between the glass electrodes are also given. These results support the experimental suggestion that the dicharge develops up to the transient glow phase and then disappears.

1. Introduction

Ozone has been used as a germicide for city water for a long time in Europe and recently utilized in various fields such as environmental pollution control, food processing or medical treatment. Ozone is usually produced by the so-called silent discharge which happens when an A. C. high voltage is applied to a gap with at least one electrode covered with a dielectric. However, the ozone yield efficiency of such a discharge device termed an ozonizer is low, which is a weak point for industrial use. Therefore, a lot of studies[1] on the silent discharge have been done to improve its efficiency, but there are very few reports which have investigated the ozone synthesis in connection with the discharge dynamics and it seems that the discharge mechanism and the ozone generation mechanism are not yet sufficiently clarified.

The authors have attempted to understand them by using a computer simulation technique. In this paper, a one-dimensional model, which can describe not only the ozone generation kinetics but also the discharge dynamics in an ozonizer with two glass electrodes, is proposed and the simulation results of the silent discharges in N_2/O_2 mixtures are presented.

---

* Presented at the National Convention Record of the I.E.E. of Japan (April 1985).

** Department of Electrical Engineering, Kitami Institute of Technology.
*** Department of Electrical Engineering, Hokkaido University.

2. Method of simulation

Generally, the silent discharge consists of a large number of discharge channels with very short duration ($\sim$10 ns) and each of the channels occurs temporally and spatially at random. A detailed simulation of the discharge appears to be a prohibitively long task. Therefore, the following assumptions have been employed in the present model.

(1) When the gap voltage V_g exceeds the discharge starting voltage V_s given previously, a single discharge with the discharge channels of N_d per unit electrode area begins to develop.

(2) The disappearance of the discharge is decided obeying the criterion that the ratio of electron current to the total discharge one becomes less than a certain value, which is usually taken as equal to 0.1.

(3) Accumulated electric charges through the discharge development are uniformly distributed on the glass surface.

The first two assumptions set limits to the discharge period, leading to a tremendous decrease in computer time. The last one allows the gap voltage to be calculated from an equivalent circuit having a series capacitor as seen in Fig. 1 (b).

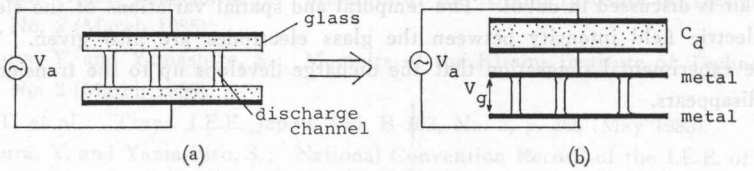

Fig. 1. (a) Schematic diagram of ozonizer gap and external circuit and (b) its equivalent circuit.

A simulation of the discharge growth in the channel, which was assumed to be identical in each case, started by releasing an initial electron pulse ($N_0=10$) from the cathode. The temporal and spatial discharge development was calculated by a similar model as in a previous work[2]. The model is based on the continuity equations for reaction species and Poisson's equation and incorporates two secondary processes; the electron emission at the cathode by positive ions and by photons. After the disappearance of the discharge was judged by the assumption (2), only the continuity equations for neutral particles were solved since the time constant of ozone generation is relatively large.

When an A. C. voltage is applied, the above procedure is repeated.

3. Reactions

The reactions listed in table 1 were taken into account, which involve the reactions between neutral particles recommended by Yagi et al.[1,3]. Furthermore, a dissociation reaction of O_2 molecules by excited nitrogen molecules $N_2(A^3\Sigma_u^+)$ and $N_2(B^3\Pi_g)$ is included as denoted by R10. It is the reaction that Filippov et al.[4] and Tabata et al[5] suggested to explain the unexpectedly high ozone yield in air. Since the rate constant of this process is not available, it is assumed

Table 1. List of reactions considered

R1	$e+O_2\rightarrow O_2^+ +2e$	R8	$e+N_2\rightarrow 2N+e$
	$+N_2\rightarrow N_2^+ +2e$	R9	$e+N_2\rightarrow N_2(C)+e$
R2	$e+O_2\rightarrow O^- +O$	R10	$e+N_2\rightarrow N_2(A)+e$
R3	$e+O_2\rightarrow O_2(B)+e\rightarrow O(^1D)+O+e$		$e+N_2\rightarrow N_2(B)+e$
R4	$e+O_2\rightarrow O_2(A)+e\rightarrow 2O+e$		$N_2(A), N_2(B)+O_2\rightarrow O(^1D)+O+N_2$
R5	$e+O_2\rightarrow O_2(b)+e$	R11	$O^- +M\rightarrow O+e+M$
R6	$e+O_2\rightarrow O_2(a)+e$	R12	$O^- +O_2\rightarrow O+O_2^-$
R7	$e+O_3\rightarrow O(^1D)+O_2(a)+e$	R13	$O_2^- +M\rightarrow e+O_2+M$
		R14	$O_2^- +M^+\rightarrow O_2+M$

S1	$O+O_2+M\rightarrow O_3+M$	S8	$O_2(a)+M\rightarrow O_2+M$	S15	$NO+O_3\rightarrow NO_2+O_2$
S2	$O+O_3\rightarrow 2O_2$	S9	$O_2(a)+O_3\rightarrow O_3+O_2$	S16	$NO+NO_3\rightarrow 2NO_2$
S3	$O+NO_2\rightarrow NO+O_2$	S10	$O_2(a)+O_3\rightarrow O+2O_2$	S17	$NO_2+O_3\rightarrow NO_3+O_2$
S4	$O+N_2O_5\rightarrow 2NO_2+O_2$	S11	$O_2(b)+M\rightarrow O_2+M$	S18	$NO_2+NO_3\rightarrow N_2O_5$
S5	$O(^1D)+O_2\rightarrow O+O_2(b)$	S12	$O_2(b)+O_3\rightarrow O+2O_2$	S19	$N_2O_5\rightarrow NO_2+NO_3$
S6	$O(^1D)+N_2\rightarrow O+N_2$	S13	$N+O_2\rightarrow NO+O$	S20	$N+NO\rightarrow N_2+O$
S7	$O(^1D)+O_3\rightarrow 2O_2$	S14	$N+O_3\rightarrow NO+O_2$		

$O_2(A)$: $O_2(A^3\Sigma_u^+)$, $O_2(B)$: $O_2(B^3\Sigma_u^-)$, $O_2(a)$: $O_2(a^1\Delta_g)$, $O_2(b)$: $O_2(b^1\Sigma_g^+)$, $N_2(A)$: $N_2(A^3\Sigma_u^+)$, $N_2(B)$: $N_2(B^3\Pi_g)$, $N_2(C)$: $N_2(C^3\Pi_u)$, $M=(O_2, N_2)$.

in the present work that all molecules of N_2 (A) and N_2 (B) dissociate O_2 instantaneously without staying in the excited states. The rate constants of the electron and the ion impact reactions R1–R14 in the table were taken from Taniguchi[6] and Badaloni et al[7], respectively and the others for the chemical reactions of neutral particles S1–S20 from reference 1.

4. Results and discussion

The computational condition was chosen from the experiment of Tanaka et al[8] who observed the light output from the silent discharges in air and oxygen of ozonizers with glass electrodes. The gap separation is 3 mm, the thickness of the glass 1.1 mm, the electrode area 4800 mm^2 and the gas pressure 760 Torr. The radius of the discharge channel, the value of N_d and the gas temperature were taken as equal to 0.375 mm, 10 cm^{-2} and 360 K, respectively according to the experimental results[1,8]. The positive ion and photon secondary ionization coefficients were assumed to be both 0.005.

4.1 Temporal variations of the gap voltage and the discharge current

Fig. 2 shows a typical wave form of the gap voltage V_g obtained by simulation under an applied voltage V_a with a frequency of 50 Hz in a mixture of 80% N_2 and 20% O_2 (hereafter referred to as air). The calculation was made on the assumption that the discharge onset field E_s/p_{20} was 50.53 $Vcm^{-1}Torr^{-1}$ (the corresponding voltage $V_s=9343$ V) and that the same discharge was intermittently repeated. The sudden drop observed in the V_g wave form corresponds to an occurrence of the single discharge with many discharge channels.

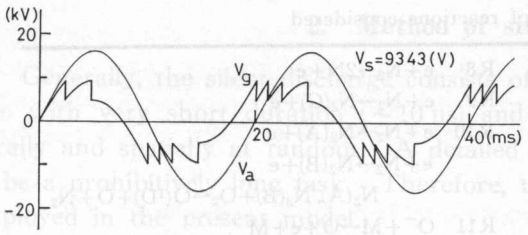

Fig. 2. Wave forms of applied voltage V_a and calculated gap voltage V_g.

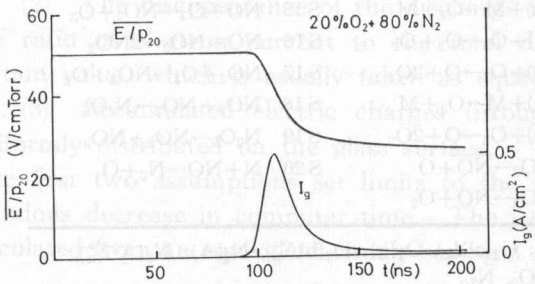

Fig. 3. Discharge current density I_g and average electric field $\overline{E/p_{20}}$ in the gap.

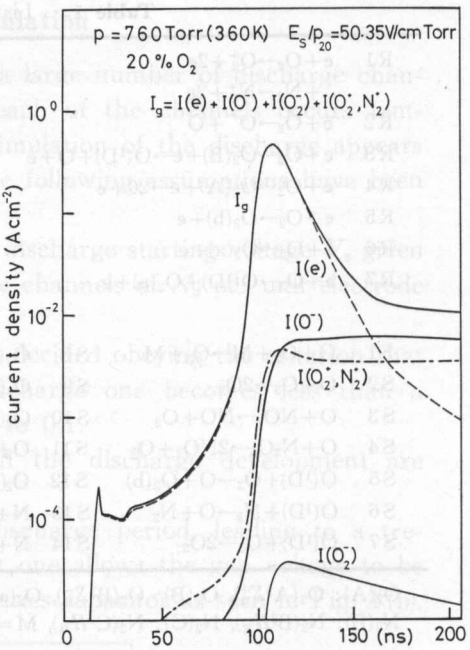

Fig. 4. Components of discharge current density I_g.

Temporally detailed variations of the voltage drop and the discharge current are shown in Fig. 3. Time zero is taken to be the instant of release of the initial electrons and an average field $\overline{E/p_{20}}$ $(=V_g/p_{20}d)$ in the gap is shown instead of V_g. The result shows that the rapid field drop accompanies a steep current pulse seen at about 110 ns. The current pulse accumulates many electric charges on the glass electrodes to lead the field drop. After the appearance of the pulse, the discharge growth is suppressed as mentioned below and it is seen that a very low current and a gentle collapse of the field follow. The current pulse width is about 16 ns, which agrees roughly with the time of discharge light output observed experimentally[8].

Fig. 4 shows components of the discharge current. It is found that the steep current pulse is formed mainly by the electron component and continuous low current at a later stage is sustained by the ion components.

4.2 Spatio-temporal growth of a silent discharge

Fig. 5 shows configurations of the electron density and the electric field intensity in the air discharge of Fig 3. The spatio-temporal development of the discharge is as follows.

The primary avalanche generated by an initial electron pulse at time zero drifts towards the anode with a long tail as seen in Fig. 5 (a) (0.6～15.2 ns). The tail is produced by successor electrons created mostly by the detachment process R11 from negative ions O^-, not by the secondary processes at the cathode.

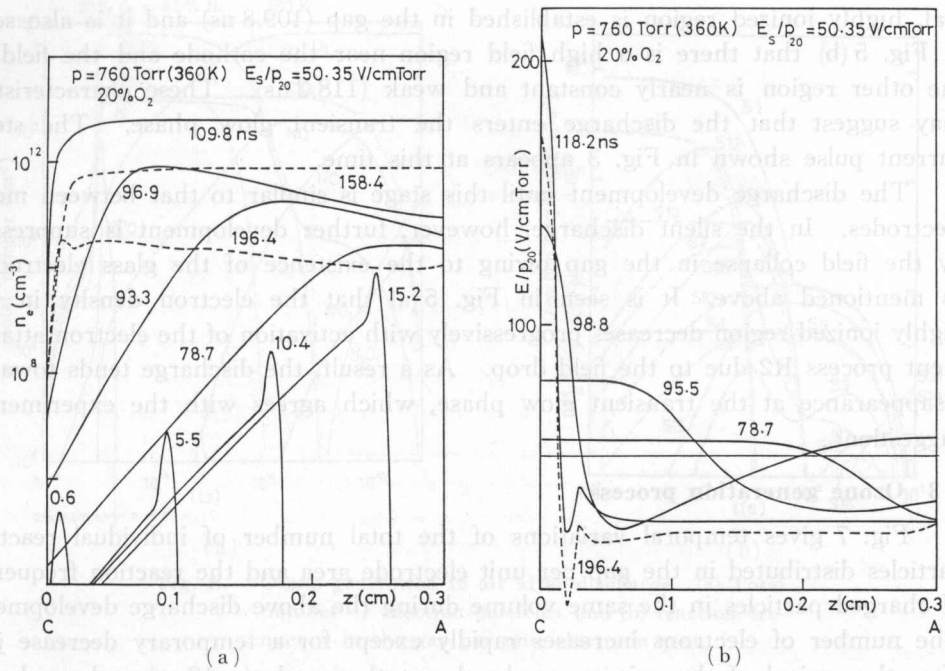

Fig. 5. Discharge development in air. (a) Electron density n_e and (b) reduced electric field E/p_{20}. C and A represent the position of the cathode and the anode, respectively.

This is clearly confirmed from comparison with Fig. 6, which gives a configuration of the electron density obtained under the same conditions as Fig. 5 except for neglecting the detachment process.

The avalanche reaches the anode at about 18 ns keeping its shape practically unchanged since the field distortion due to the space charges does not appear yet. However, it is observed in Fig. 5 (b) that a high field region appears in the cathode side at 78.7 ns. The high field, which is formed by positive space charges accumulated in front of the anode owing to the continuous arrival of successor avalanches, enhances ionization in the low ionized region of the cathode side. As a result, a rapid discharge development towards the cathode, namely the so-called cathode-directed streamer, is observed (78.7～96.9 ns). After this development, a quasineu-

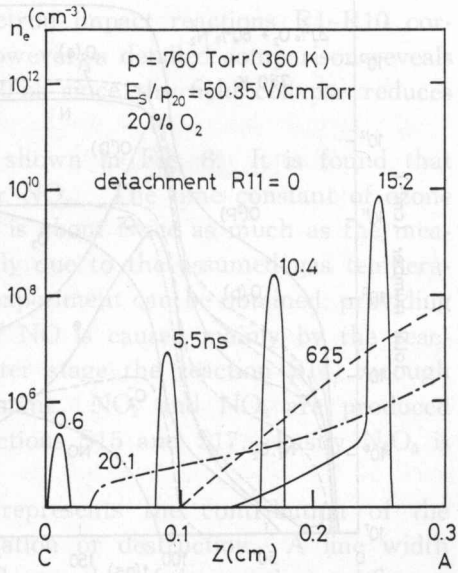

Fig. 6. Configuration of electron density n_e, provided that the detachment reaction R11 is neglected.

tral, highly ionized region is established in the gap (109.8 ns) and it is also seen in Fig. 5 (b) that there is a high field region near the cathode and the field in the other region is nearly constant and weak (118.2 ns). These characteristics may suggest that the discharge enters the transient glow phase. The steep current pulse shown in Fig. 3 appears at this time.

The discharge development until this stage is similar to that between metal electrodes. In the silent discharge, however, further development is suppressed by the field collapse in the gap owing to the existence of the glass electrodes, as mentioned above. It is seen in Fig. 5 (a) that the electron density in the highly ionized region decreases progressively with activation of the electron attachment process R2 due to the field drop. As a result, the discharge tends towards disappearance at the transient glow phase, which agrees with the experimental suggestion[9].

4.3 Ozone generation process

Fig. 7 gives temporal variations of the total number of individual reaction particles distributed in the gap per unit electrode area and the reaction frequency of charged particles in the same volume during the above discharge development. The number of electrons increases rapidly except for a temporary decrease just after the arrival of the primary avalanche at the anode ($\sim$18 ns) and reaches a maximum when the transient glow discharge is established ($\sim$110 ns). After that, the number decreases with the field collapse. A similar variation is observed in

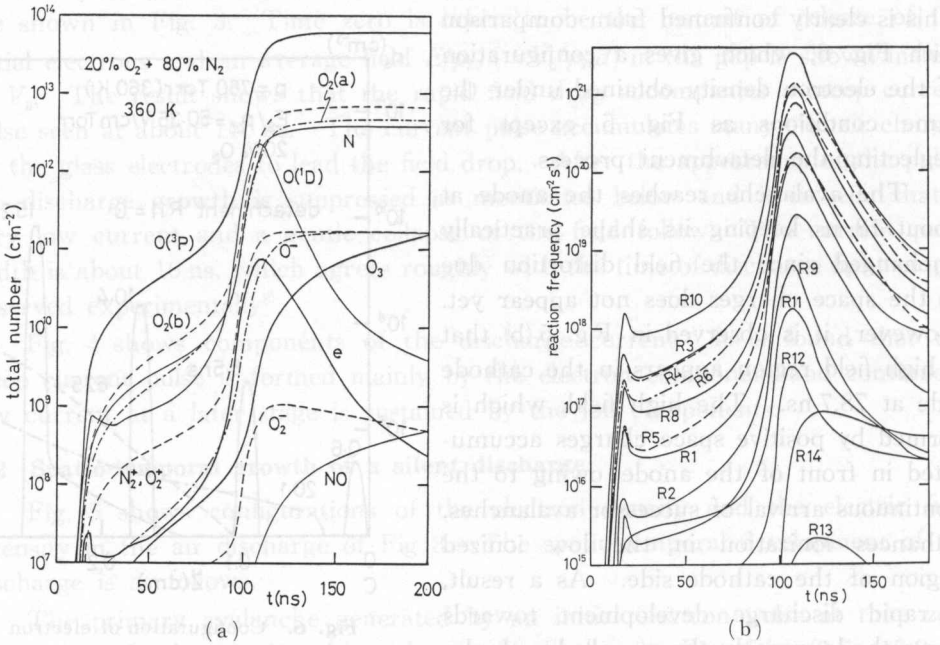

Fig. 7. Ozone generation in air during discharge period. (a) Total number of reaction particles and (b) reaction frequency in the gap per unit electrode area.

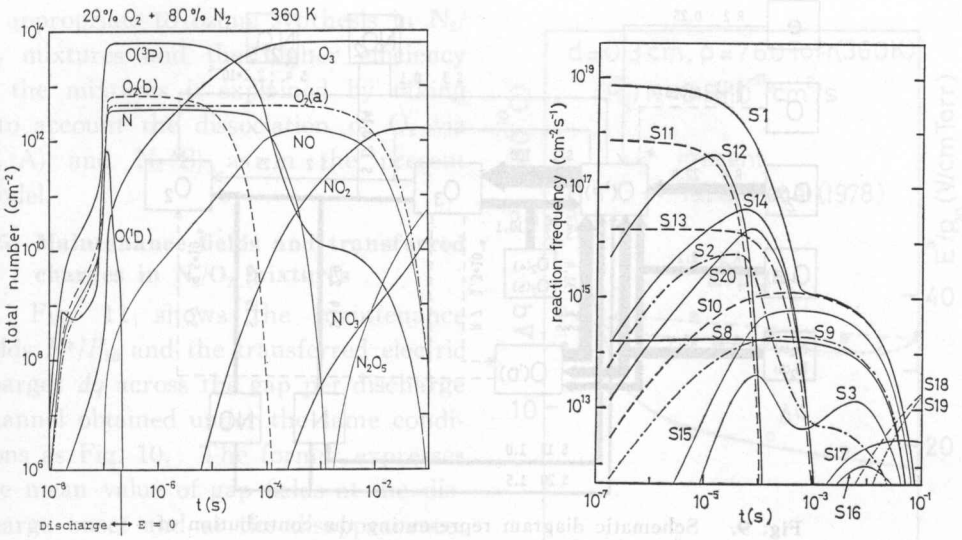

Fig. 8. Ozone generation in air after discharge. (a) Total number of reaction particles and (b) reaction frequency in the gap per unit electrode area.

the result for $O(^1D)$. On the other hand, atomic oxygens $O(^3P)$, which produce almost exclusively O_3 through the reaction S1, are rapidly generated and become saturated with the decrease of the electron number. Such a variation is recognized in the growth of $O_2(a^1\Delta_g)$, $O_2(b^1\Sigma_g^+)$ and atomic nitrogens N.

The variations of the frequency of electron impact reactions R1–R10 correspond to that of the electron number. However, a detailed comparison reveals a faster decrease in the frequency at $t>110$ ns since the field collapse reduces the rate constant too.

The variations after the discharge are shown in Fig. 8. It is found that O_3 and NO are produced ahead of the other NO_x. The time constant of ozone generation in the Fig. is about 36 μs, which is about twice as much as the measured one[10]. This difference may be partially due to the assumed gas temperature (360 K), since good agreement with the experiment can be obtained, providing the temperature is 300 K. The synthesis of NO is caused mainly by the reaction S13 at the early stage, while at the later stage the reaction S14, through which O_3 is decomposed, becomes predominant. NO_2 and NO_3 are produced subsequently through the O_3 destruction reactions S15 and S17. Lastly N_2O_5 is synthesized by the reaction S18.

Fig. 9 is a schematic picture which represents the contribution of the individual reaction particles to the O_3 generation or destruction. A line width drawn in the Fig. is selected in proportion to the number of the reaction and figures along the line indicate the percentage of the number of each reaction to that of S1. Taking into account the contribution through $O(^1D)$, the contribution of excited nitrogen molecules $N_2(A)$ and $N_2(B)$ is about 47%, which is comparable

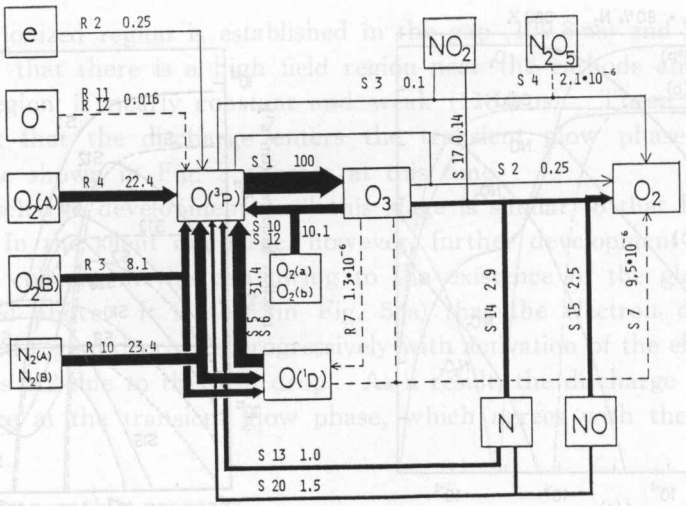

Fig. 9. Schematic diagram representing the contribution of reaction particle to ozone generation or destruction.

with that of the excited oxygen molecules O_2(A) and O_2(B), 49%. This result suggests that the optimum ozone yield in air becomes roughly twice as much as the value inferred from only the O_2 fraction, which agrees with experimental results. It can also be pointed out from the Fig. that destruction of O_3 by N and NO is dominant in a dilute ozone concentration as in the present work.

4.4 Ozone yield efficiencies in N_2/O_2 mixtures

Further calculations to examine the validity of the present model were performed in various mixtures of N_2 and O_2. Fig. 10 shows the efficiencies of ozone yield obtained by a single discharge. In the calculation, the value of the discharge onset field in each mixture was chosen to give the same effective ionization frequency ($\overline{R_i}/N=3.5\times10^{-11}\,\mathrm{cm^3s^{-1}}$) as a similar discharge development was expected. Moreover, the relative efficiency was estimated providing that an ozone yield obtained in a calculation considering only the reactions in O_2 was proportional to a partial pressure of O_2, since the present calculation could not give the exact electric energy of the discharge owing to the assumption (2) in section 2. The calculated efficiency is in excellent agreement with the measurements[5,10] in the whole mixtures. This result may conclude that the present model

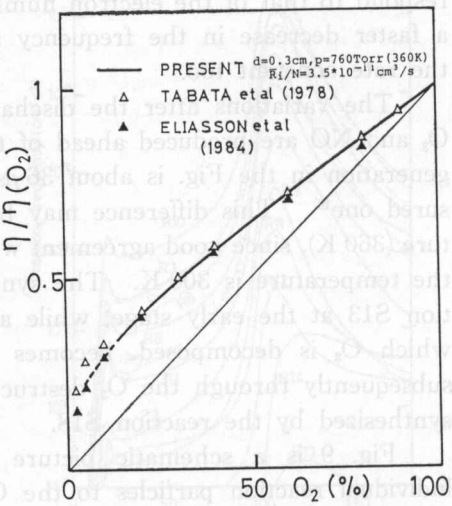

Fig. 10. Relative efficiency of ozone yield in N_2/O_2 mixtures. $\eta(O_2)$ denotes the yield efficiency in oxygen.

is appropriate to ozone synthesis in N_2/O_2 mixtures and the higher efficiency in the mixtures is explained by taking into account the dissociation of O_2 via $N_2(A)$ and $N_2(B)$ as in the present model.

4.5 Maintenance fields and transferred charges in N_2/O_2 mixtures

Fig. 11 shows the maintenance fields E^*/P_{20} and the transferred electric charges Δq across the gap per discharge channel obtained under the same conditions as Fig. 10. The former expresses the mean value of gap fields at the discharge onset and at the disappearance. Although the assumption was made for the disappearance of the discharge, the calculated fields are in rather good agreement with the measured ones[5] and the transferred charges are consistent with the experiment[8] which reports charges of 10^{-9}C order in air and 10^{-10}C order in oxygen. It may be suggested from these results that the present discharge model on the assumption is reasonable.

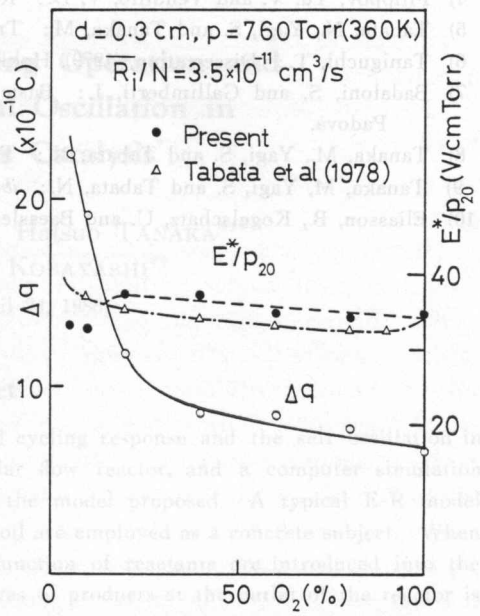

Fig. 11. Discharge maintenance field E^*/p_{20} and transferred electric charges Δq per discharge channel in N_2/O_2 mixtures.

5. Conclusions

A model which simulates a silent discharge in N_2/O_2 mixtures has been proposed in the present paper. The ozone yield efficiency and the maintenance electric field obtained by the model agree well with the experiments, which may support the validity of the present model.

It has been pointed out that the unexpectedly high efficiency of ozone yield in N_2/O_2 mixtures is caused by dissociation of O_2 by excited nitrogen molecules $N_2(A^3\Sigma_u^+)$ and $N_2(B^3\Pi_g)$. It has also been clarified that although the discharge development up to the establishment of the transient glow is similar to that between metal electrodes, the subsequent development is rapidly suppressed due to the electric charges accumulated on the glass electrodes by a steep current pulse.

References

1) Technical Report of the IEE Japan, Part II, No. 127, (1982), the IEE Japan.
2) Yoshida, K. and Tagashira, H.: Journal of the Japan Research Group of Electrical Discharge, No. 95, 50 (1983).
3) Yagi, S. and Tanaka, M.: J. Phys. D, **12**, 1509 (1979).

4) Filippov, Yu. V. and Vendillo, V. D.: Russ. J. Phys. Chem., **36**, 1069 (1962).
5) Tabata, N., Yagi, S. and Tanaka, M: Trans. IEE Japan, **98B**, 123 (1978).
6) Taniguchi, T.: Dissertation, (1979), Hokkaido University.
7) Badaloni, S. and Gallimberti, I.: Basic Data of Air Discharges, (1972), Universita' di Padova.
8) Tanaka, M., Yagi, S. and Tabata, N.: Trans. IEE Japan, **98A**, 57 (1978).
9) Tanaka, M, Yagi, S. and Tabata, N.: *ibid.*, **102A**, 553 (1982).
10) Eliasson, B., Kogelschatz, U. and Baessler, P.: J. Phys. B, **17**, L797 (1984).